J. Fluid Mech. (1984), *vol.* 147, *pp.* 213–231
Printed in Great Britain

Internal solitary waves and their head-on collision. Part 1

By RIDA M. MIRIE
Department of Mathematical Sciences, University of Petroleum and Minerals, Dhahran, Saudi Arabia

AND C. H. SU
Division of Applied Mathematics, Brown University, Providence, R.I. 02912, U.S.A.

(Received 18 July 1983 and in revised form 9 May 1984)

Head-on collision of two (KdV) solitary waves at the interface of an inviscid two-fluid system of rigid upper and lower boundaries is investigated by a perturbation method. We obtain the third-order solution and find a dispersive wavetrain trailing behind each emerging solitary wave. The wavetrain is of the same polarity (depression/elevation) as the main wave. Furthermore, the energy and amplitude of the wavetrain are decreasing in time as long as it is still attached to the main wave. This implies an increase in energy of the main wave. Up to the third order of accuracy the solitary wave emerging from a head-on collision retains its initial profile save for a phase shift. This phase shift is found to be amplitude dependent to the second order. The transfer of energy from the wavetrain to the main wave explains the slow recovery of the incident profiles in existing numerical results on the head-on collision of two solitary waves at the surface of an infinite channel.

1. Introduction

Recently many authors have investigated the solitary wave at the interface of an inviscid two-fluid system of rigid upper and lower boundaries. For reviews see Miles (1980), Koop & Butler (1981), Segur & Hammack (1982) and Gear & Grimshaw (1983).

In this paper we consider the head-on collision of two solitary waves by a perturbation method to the third order. In §2 we present the equations of motion in terms of horizontal bottom and ceiling velocities, and the interface. A change to the characteristic variables $(\xi, \eta, \alpha, \beta)$ renders the problem virtually identical with that of the head-on collision at the surface of an infinite channel. In the limit as the density of the upper fluid layer goes to zero, the solution obtained agrees with that of Su & Mirie (1980, hereinafter referred to as paper 1).

The KdV equation describes the solitary wave in the first order of approximation. This wave is of depression (or elevation) if σ is greater (or smaller) than R^2, where σ denotes the ratio of the fluid densities and R^2 denotes the square of the ratio of depths of the fluid layers. The second-order solution of a solitary wave agrees with that of Koop & Butler (1981). See Appendix B. The third-order solution of the head-on collision indicates that an emergent solitary wave is tilted backwards to its direction of propagation. We obtain third-order results in the run up (maximum amplitude during the interaction) and the wave speed. The second-order phase shift is classified into uniform and non-uniform shifts. The latter causes the emergent wave to tilt backwards to its direction of propagation.

The study of the slow time evolution of an emergent wave (asymmetric) is similar to that of paper 1. We find that the emergent wave evolves into a symmetric solitary wave that is trailed by a dispersive wavetrain with its head wave having the same polarity (depression/elevation) of the solitary wave. We also show that the energy of the wavetrain decreases in time as long as it is not entirely separated from the main wave. Since the energy of the entire system is conserved, this implies a transfer of energy from the wavetrain to the main wave before they completely separated.

In the limit as the density of the upper layer goes to zero, the head-on collision problem considered is equivalent to that at the free surface of an infinite channel. In §3 we discuss the recent numerical results on the latter problem. The results discussed are those of Mirie & Su (1982), Funakoshi & Oikawa (1982) and Fenton & Rienecker (1982).

A head-on collision between two solitary waves can be considered as made up of two parts: the first part (in a faster timescale) is characterized by the interaction of two main waves; the second part consists of generation of secondary waves for each main wave while the two main waves are already separated from each other. The second part also involves the slow separation of the secondary wave from its parent wave. From the numerical results cited above, it is found that the amplitude of the wave right at the end of the first part of the collision is smaller than that of the incoming wave. However, there is a recovery of the deficit in amplitude during the second part of the collision. From the theoretical and numerical results, the final deficit is smaller than the third order in the amplitude parameter.

2. The perturbation method and results

We consider two immiscible, inviscid, homogeneous fluids bounded from above and below by two rigid horizontal planes. The densities of the lower and upper fluids are ρ_1 and ρ_2 with $\sigma = (\rho_2/\rho_1) < 1$. When undisturbed the fluids lie in uniform layers of depths h_0 and $H-h_0$ respectively.

Let W_1 and W_2 represent the horizontal velocities at the bottom and the ceiling respectively, while $h(x,t)$ represents the interface measured from the bottom. We present the continuity equation in the lower and upper fluid layers, and the Bernoulli equation at the interface (see Mirie 1980) as

$$h_t + \left[\sum_0^\infty \frac{(-1)^n h^{2n+1}}{(2n+1)!}\partial_x^{2n} W_1\right]_x = 0, \tag{1}$$

$$h_t + \left[\sum_0^\infty \frac{(-1)^n (h-H)^{2n+1}}{(2n+1)!}\partial_x^{2n} W_2\right]_x = 0 \tag{2}$$

and

$$\begin{aligned}[W_1 - \sigma W_2]_t + \Bigg[(1-\sigma)gh + \tfrac{1}{2}(W_1^2 - \sigma W_2^2) + \sum_1^\infty \frac{(-1)^n h^{2n}}{(2n)!} \\ \times \left[\partial_t \partial_x^{2n-1} W_1 + \frac{1}{2}\sum_0^{2n} (-1)^m C_m^{2n} \partial_x^m W_1 \partial_x^{2n-m} W_1\right] \\ - \sigma \sum_1^\infty \frac{(-1)^n (h-H)^{2n}}{(2n)!}\left[\partial_t \partial_x^{2n-1} W_2 + \tfrac{1}{2}\sum_0^{2n} (-1)^m C_m^{2n} \partial_x^m W_2 \partial_x^{2n-m} W_2\right]\Bigg]_x = 0,\end{aligned} \tag{3}$$

where g is the acceleration due to gravity and $C_m^{2n} = \binom{2n}{m}$ is the binomial coefficient. Equations (1) and (3) reduce to those of paper 1 for the case $\sigma = 0$.

We consider two interfacial solitary waves, far apart, of small but finite amplitude, heading towards each other. Our purpose is to study the phase shift, maximum wave height and the generation of secondary waves (wavetrain) of a collision of two such solitary waves. For this purpose we shall introduce changes in the independent and dependent variables, which will facilitate the direct application of the perturbation method of paper 1. We take

$$\left.\begin{aligned}\xi &= \epsilon^{\frac{1}{2}}K(x-C_{\mathrm{R}}t)+\epsilon K\theta(\xi,\eta),\\ \eta &= \epsilon^{\frac{1}{2}}L(x+C_{\mathrm{L}}t)+\epsilon L\psi(\xi,\eta),\end{aligned}\right\} \tag{4}$$

where $0<\epsilon\ll 1$ is a dimensional parameter of the order of amplitude of the wave. The wavenumbers K and L of the right- and left-going waves are of order unity. The wave speeds C_{R} and C_{L} of the right- and left-going waves are related to the amplitude of the corresponding waves. For infinitesimal amplitudes C_{R} and C_{L} reduce to the linear speed $C^2=gh_0(1-\sigma)/(1-\sigma/R)$, where $R=1-H/h_0$ is equivalent to $-r$ (the parameter used initially by Long 1956).

The transformation between derivatives is given by equations (12) and (13) of paper 1. Letting $h=h_0(1+\zeta)$, we introduce the following change of dependent variables:

$$\zeta=\epsilon(\alpha+\beta), \tag{5a}$$

$$W=\epsilon(\alpha-\beta), \tag{5b}$$

$$W_1=W+\epsilon^2\sigma p, \tag{5c}$$

$$W_2=W/R+\epsilon^2 p. \tag{5d}$$

The new variables are then expanded in the following power series:

$$\left.\begin{aligned}p &= p_0(\xi,\eta)+\epsilon p_1(\xi,\eta)+\ldots,\\ \alpha &= \alpha_0(\xi)+\epsilon\alpha_1(\xi,\eta)+\epsilon^2\alpha_2(\xi,\eta)+\ldots,\\ \beta &= \beta_0(\eta)+\epsilon\beta_1(\xi,\eta)+\epsilon^2\beta_2(\xi,\eta)+\ldots,\\ \theta &= \theta_0(\eta)+\epsilon\theta_1(\xi,\eta)+\ldots,\\ \psi &= \psi_0(\xi)+\epsilon\psi_1(\xi,\eta)+\ldots,\\ C_{\mathrm{R}}/C &= 1+\epsilon a\lambda_1+\epsilon^2a^2\lambda_2+\epsilon^3a^3\lambda_3+\ldots,\\ C_{\mathrm{L}}/C &= 1+\epsilon b\lambda_1+\epsilon^2b^2\lambda_2+\epsilon^3b^3\lambda_3+\ldots,\end{aligned}\right\} \tag{6}$$

where a and b are of order of the amplitude of the right- and left-going solitary waves. We also use the following notation:

$$D_1=1-\frac{\sigma}{R},\quad D_2=1-\frac{\sigma}{R^2},\quad R_1=1-\frac{1}{R},\quad R_2=R(R+1),\quad R_3=R^3-\sigma,$$

$$U=1-\sigma R,\quad U_3=1-\sigma R^3,\quad \sigma_1=\sigma-1,\quad \Omega_1=\frac{\sigma R_1^2}{RU^2D_2^2},$$

$$\gamma_2(m_1,m_2,m_3)=m_1R_2^2D_2^2+m_2R_2D_2U+m_3U^2,$$

$$\gamma_4(m_1,m_2,m_3,m_4,m_5)=m_1R_2^4D_2^4+m_2R_2^3D_2^3U+m_3R_2^2D_2^2U^2+m_4R_2D_2U^3+m_5U^4, \tag{7}$$

where the m_i are rational numbers to be given later.

Subtracting (2) from (1) and then substituting the expansions (6), we determine the p_n as

$$p_0=\frac{R_1}{RD_1}[\alpha_0^2-\beta_0^2+\tfrac{1}{6}R_2h_0^2(K^2\alpha_{0\xi\xi}-L^2\beta_{0\eta\eta})] \tag{8}$$

and
$$p_1 = \frac{1}{RD_1}[2R_1(\alpha_0\alpha_1 - \beta_0\beta_1) - \sigma_1(\alpha_0+\beta_0)p_0$$
$$+\tfrac{1}{6}h_0^2(K^2\partial_\xi^2 + L^2\partial_\eta^2)(R_1R_2(\alpha_1-\beta_1)+R_3p_0)$$
$$+\tfrac{1}{6}R_1R_2KLh_0^2(2K\theta_{0\eta}\alpha_{0\xi\xi} - 2L\psi_{0\xi}B_{0\eta\eta} + K\theta_{0\eta\eta}\alpha_{0\xi} - L\psi_{0\xi\xi}\beta_{0\eta})$$
$$+\tfrac{1}{2}RR_1h_0^2(\alpha_0+\beta_0)(K^2\alpha_{0\xi\xi} - L^2\beta_{0\eta\eta}) - \frac{h_0^4}{5!}(R^4-1)(K^4\alpha_{0\xi\xi\xi\xi} - L^4\beta_{0\eta\eta\eta\eta})].$$

Now substituting (6), p_0 and p_1 in [eqn (3) $\pm$ (eqn (1) $-(\sigma/R)$ eqn (2))], we obtain equations for α and β respectively. The equation for α is given in Appendix A. The equation for β can be obtained from that for α by replacing α by β, ξ by η, K by L, F_+ by F_- and θ by ψ. Hence we need only consider the equation for α. Consequently the method of solution coincides with that of paper 1.

2.1. *Method of solution*

We summarize the method of solution by considering only the coefficients of ϵ^2 in the equation for α. The solution for the higher orders of ϵ follows steps identical with those of ϵ^2. We have

$$4D_1L\alpha_{1\eta} + aK[\tfrac{1}{3}K^2h_0^2Uf'' + \tfrac{3}{2}aD_2f^2 - 2\lambda_1aD_1f]_\xi$$
$$+aKf'[4LD_1\theta_{0\eta} - D_2bg] + L[D_2(abfg - b^2g^2) + \tfrac{2}{3}L^2h_0^2Ubg'']_\eta = 0. \quad (9)$$

We classify the terms in the successive brackets to be secular, non-local and local respectively. The secular terms are independent of η. If they were integrated with respect to η, they would produce an unbounded solution for α_1. Thus we set them equal to zero and obtain

$$[\tfrac{1}{3}Uh_0^2K^2f'' + \tfrac{3}{2}aD_2f^2 - 2\lambda_1aD_1f]_\xi = 0, \quad (10)$$

where $f = \alpha_0(\xi)/a$. The coefficient $D_2 = 1 - \sigma/R^2$ in front of f^2 above is just the parameter derived by Long (1956). This parameter determines the polarity of the KdV soliton profile, i.e. the wave is of depression or elevation according to whether $\sigma > R^2$ or $\sigma < R^2$. For $\sigma = R^2$ the nonlinear terms disappear. Thus we consider $\sigma \neq R^2$ throughout this paper. In the case where D_2 is of the order of magnitude of the amplitude, we have cubic as well as quadratic nonlinearity, which will be treated in a separate article. (See also Kakutani & Yamasaki (1978), Miles (1979, 1980) and Gear & Grimshaw (1983).) We let

$$h_0^2K^2 = \frac{3aD_2}{U}, \quad \lambda_1 = \frac{\frac{1}{2}D_2}{D_1}, \quad h_0^2L^2 = \frac{3bD_2}{U}. \quad (11)$$

Then the solitary-wave solution for f is given by

$$f = S(\xi) = \operatorname{sech}^2\tfrac{1}{2}\xi, \quad (12)$$

and similarly
$$g = S(\eta) = \operatorname{sech}^2\tfrac{1}{2}\eta. \quad (13)$$

Since K is real as defined in (4), we see from (11) that for $D_2 < 0$ (or > 0) we have $a < 0$ (or > 0), corresponding to a wave of depression (or elevation).

The non-local terms determine the phase function θ_0 as a $2\lambda_1$ multiple of the results of Oikawa & Yajima (1973) for the case $\sigma = 0$.

The local terms when integrated with respect to η determine α_1 up to an arbitrary function $F_1(\xi)$. The latter is determined from the secular terms in the ϵ^3 order. The method of solution is then carried to the next orders of ϵ. The function $F_2(\xi)$ resulting

from integrating α_2 is determined in the ϵ^4 order (see Appendix A). Consequently we complete the third-order solution in terms of ϵ. An exact relation for C_R in terms of ϵ can be obtained from the linearized terms of (1)–(3). This relation provides a check on the calculation in the ϵ-notation. We have

$$h_0 k \frac{C_R^2}{C^2} = \frac{D_1}{\cot(h_0 k) - \sigma \cot(h_0 k R)}, \tag{14}$$

where $h_0 k$ is given by (11).

2.2. *Third-order results*

We now recast the third-order solution in terms of the amplitude expansion parameters $\epsilon_R = \zeta(f=1, g=0)$ and $\epsilon_L = \zeta(f=0, g=1)$ of the right- and left-going solitary waves. Expressions for the variables relevant to the left-going wave could be obtained from those listed below by replacing a by b, ϵ_R by ϵ_L, ξ by η, and f by g.

The parameter of expansion $a\epsilon$ is related to ϵ_R by

$$a\epsilon = \epsilon_R + (2\lambda_1)\epsilon_R^2 T_1 + (2\lambda_1)^2 \epsilon_R^3 T_2, \tag{15}$$

where

$$T_1 = -\tfrac{5}{4} + \Omega_1 \gamma_2(\tfrac{1}{4}, 0, 1)$$

and

$$T_2 = \tfrac{3}{2} + \Omega_1 \Big[\gamma_2\Big(-\frac{59}{80}, -\frac{3}{5}, -\frac{61}{20}\Big) + \frac{R_3}{RU}\gamma_2\Big(0, \frac{11}{80}, \frac{3}{5}\Big) + \frac{RD_1}{U}\gamma_2\Big(0, \frac{17}{80}, \frac{3}{20}\Big) + \frac{\sigma_1}{RD_2}\gamma_2\Big(\frac{3}{20}, -\frac{9}{20}, 1\Big) + \Omega_1 \gamma_4\Big(\frac{1}{20}, \frac{1}{10}, \frac{3}{5}, 0, 0\Big)\Big].$$

The wave speed of the right-going wave is given by

$$\frac{C_R}{C} = 1 + \lambda_1 \epsilon_R + (2\lambda_1)^2 \epsilon_R^2 T_3 + (2\lambda_1)^3 \epsilon_R^3 T_4, \tag{16}$$

where

$$T_3 = -\tfrac{3}{20} + \Omega_1 \gamma_2(\tfrac{1}{40}, 0, \tfrac{1}{2})$$

and

$$T_4 = \tfrac{3}{56} + \Omega_1 \Big[\gamma_2\Big(-\frac{99}{1120}, -\frac{3}{10}, -\frac{23}{40}\Big) + \frac{R_3}{RU}\gamma_2\Big(-\frac{1}{35}, \frac{11}{160}, \frac{3}{10}\Big) + \frac{RD_1}{U}\gamma_2\Big(0, \frac{17}{160}, \frac{3}{40}\Big) + \frac{\sigma_1}{RD_2}\gamma_2\Big(\frac{3}{40}, -\frac{9}{40}, \frac{1}{2}\Big) + \Omega_1 \gamma_4\Big(-\frac{1}{40}, \frac{1}{20}, \frac{1}{10}, 0, 0\Big)\Big].$$

On replacing R by $-r$, the second-order speed agrees with that of Long (1956). In Appendix B we compare the second-order solution to that of Koop & Butler (1981), which has been confirmed by Gear & Grimshaw (1983). In figure 1 we plot C_R versus the amplitude for $R = -2.5$ and several values of σ.

The wavenumber of the right-going wave is given by

$$h_0 K = \Big(\frac{3\epsilon_R D_2}{U}\Big)^{\frac{1}{2}} [1 + 2\lambda_1 \epsilon_R T_5 + (2\lambda_1 \epsilon_R)^2 T_6], \tag{17}$$

where

$$T_5 = -\tfrac{5}{8} + \Omega_1 \gamma_2\Big(\frac{1}{8}, 0, \frac{1}{2}\Big)$$

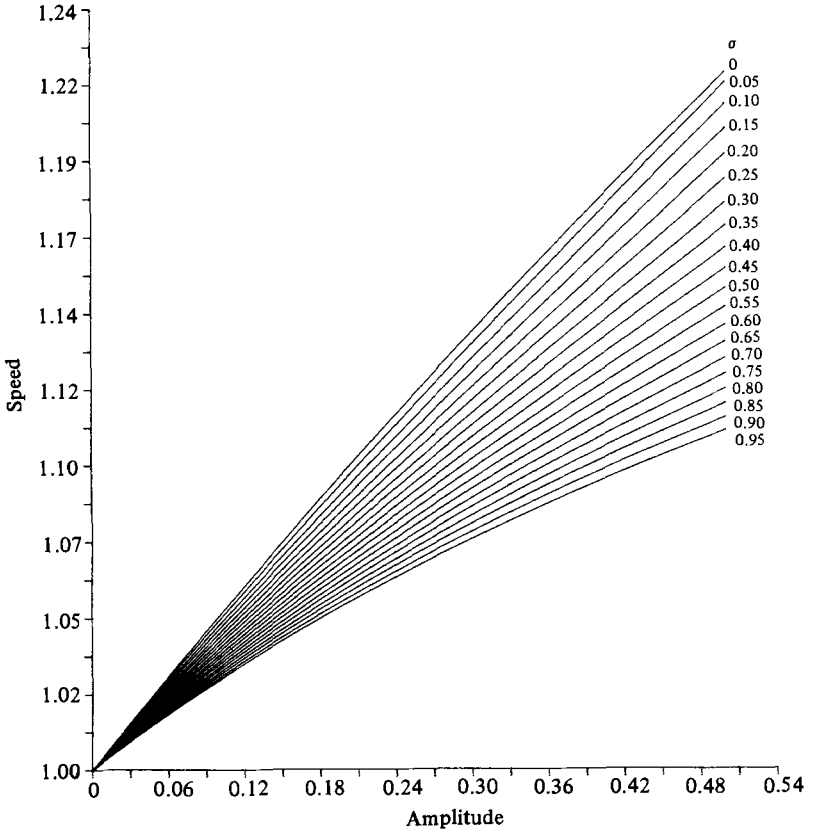

FIGURE 1. The third-order result for the wave speed of an internal solitary wave versus the wave amplitude for $R = -2.5$ and several values of σ.

and

$$T_6 = \tfrac{71}{128} + \Omega_1\Big[\gamma_2\Big(-\frac{93}{320}, -\frac{3}{10}, -\frac{97}{80}\Big) + \frac{R_3}{RU}\gamma_2\Big(0, \frac{11}{160}, \frac{3}{10}\Big) + \frac{RD_1}{U}\gamma_2\Big(0, \frac{17}{160}, \frac{3}{40}\Big) + \frac{\sigma_1}{RD_2}\gamma_2\Big(\frac{3}{40}, -\frac{9}{40}, \frac{1}{2}\Big) + \Omega_1\gamma_4\Big(\frac{11}{640}, \frac{1}{20}, \frac{19}{80}, 0, -\frac{1}{8}\Big)\Big].$$

The interface displacement is given by

$$\begin{aligned}\zeta = {} & [\epsilon_R + 2\lambda_1 T_7 \epsilon_R^2 f(f-1) + (2\lambda_1)^2 \epsilon_R^3 f(T_8 f^2 + T_9 f + T_{10})] \\ & + [\epsilon_L + 2\lambda_1 T_7 \epsilon_L^2 g(g-1) + (2\lambda_1)^2 \epsilon_L^3 g(T_8 g^2 + T_9 g + T_{10})] \\ & + 2\lambda_1 \epsilon_L \epsilon_R fg[\tfrac{1}{2} + 2\lambda_1(T_{11}(\epsilon_R f + \epsilon_L g) + T_{12}(\epsilon_R + \epsilon_L))],\end{aligned} \tag{18}$$

where

$$T_7 = \tfrac{3}{4} + \Omega_1\gamma_2(-\tfrac{3}{4}, 1, 1),$$

$$T_8 = \tfrac{101}{80} + \Omega_1\Big[\gamma_2\Big(-\frac{13}{40}, \frac{589}{240}, \frac{46}{15}\Big) + \frac{R_3}{RU}\gamma_2\Big(\frac{3}{5}, -\frac{21}{20}, -\frac{7}{15}\Big) + \frac{RD_1}{U}\gamma_2\Big(0, -\frac{81}{80}, -\frac{17}{10}\Big) + \frac{\sigma_1}{RD_2}\gamma_2\Big(-\frac{81}{80}, \frac{11}{10}, \frac{1}{3}\Big) + \Omega_1\gamma_4\Big(\frac{93}{80}, -\frac{51}{20}, -\frac{29}{30}, \frac{7}{3}, 1\Big)\Big],$$

$$T_9 = -\tfrac{151}{80} + \Omega_1\Big[\gamma_2\Big(\frac{131}{80}, -\frac{719}{240}, -\frac{119}{60}\Big) + \frac{R_3}{RU}\gamma_2\Big(-\frac{3}{5}, \frac{79}{80}, \frac{2}{15}\Big)$$
$$+ \frac{RD_1}{U}\gamma_2\Big(0, \frac{39}{20}, -\frac{31}{20}\Big) + \frac{\sigma_1}{RD_2}\gamma_2\Big(\frac{31}{80}, \frac{13}{20}, \frac{4}{3}\Big) + \Omega_1\gamma_4\Big(-\frac{123}{80}, \frac{61}{20}, \frac{19}{30}, -\frac{11}{3}, -3\Big)\Big],$$

$$T_{10} = \tfrac{5}{8} + \Omega_1\Big[\gamma_2\Big(-\frac{21}{16}, \frac{13}{24}, -\frac{13}{12}\Big) + \frac{R_3}{RU}\gamma_2\Big(0, \frac{1}{16}, \frac{1}{3}\Big)$$
$$+ \frac{RD_1}{U}\gamma_2\Big(0, -\frac{15}{16}, \frac{13}{4}\Big) + \frac{\sigma_1}{RD_2}\gamma_2\Big(\frac{5}{8}, -\frac{7}{4}, -\frac{5}{3}\Big) + \Omega_1\gamma_4\Big(\frac{3}{8}, -\frac{1}{2}, \frac{1}{3}, \frac{4}{3}, 2\Big)\Big],$$

$$T_{11} = \tfrac{7}{4} + \Omega_1\gamma_2\Big(-\frac{3}{8}, \frac{19}{8}, 1\Big)$$

and

$$T_{12} = -\tfrac{11}{8} + \Omega_1\gamma_2\Big(\frac{3}{8}, -\frac{7}{4}, -\frac{1}{2}\Big).$$

The third-order solitary-wave solution can be obtained from (18) by setting $g = 0$. To the second order it agrees with that of Koop & Butler (1981) (see Appendix B). In figure 2 we plot this solution for amplitude 0.31 versus ξ and σ. As σ increases, the wave becomes flatter.

The horizontal bottom and ceiling velocities are represented by the function W as defined in (5*b*). We have:

$$W = \epsilon_R f - \epsilon_L g + 2\lambda_1[T_{13}(\epsilon_R^2 f - \epsilon_L^2 g) + T_{14}(\epsilon_R^2 f^2 - \epsilon_L^2 g^2)]$$
$$+ (2\lambda_1)^2[\epsilon_R^3(T_{15}f^3 + T_{16}f^2 + T_{17}f) - \epsilon_L^3(T_{15}g^3 + T_{16}g^2 + T_{17}g)$$
$$+ \epsilon_R\epsilon_L fg(T_{18}(\epsilon_R f - \epsilon_L g) + T_{19}(\epsilon_R - \epsilon_L))], \tag{19}$$

where

$$T_{13} = \tfrac{1}{4} + \Omega_1\gamma_2(\tfrac{3}{4}, -1, 1),$$

$$T_{14} = -1 + \Omega_1\gamma_2(-\tfrac{3}{4}, 1, 1),$$

$$T_{15} = \tfrac{6}{5} + \Omega_1\Big[\gamma_2\Big(\frac{139}{80}, -\frac{251}{240}, -\frac{73}{30}\Big) + \frac{R_3}{RU}\gamma_2\Big(\frac{3}{5}, -\frac{21}{20}, -\frac{7}{15}\Big)$$
$$+ \frac{RD_1}{U}\gamma_2\Big(0, -\frac{81}{80}, -\frac{17}{10}\Big) + \frac{\sigma_1}{RD_2}\gamma_2\Big(-\frac{81}{80}, \frac{11}{10}, \frac{1}{3}\Big) + \Omega_1\gamma_4\Big(\frac{93}{80}, -\frac{51}{20}, -\frac{29}{30}, \frac{7}{3}, 1\Big)\Big],$$

$$T_{16} = -\tfrac{1}{5} + \Omega_1\Big[\gamma_2\Big(-\frac{47}{40}, \frac{301}{240}, \frac{151}{60}\Big) + \frac{R_3}{RU}\gamma_2\Big(-\frac{3}{5}, \frac{79}{80}, \frac{2}{15}\Big)$$
$$+ \frac{RD_1}{U}\gamma_2\Big(0, \frac{39}{20}, -\frac{31}{20}\Big) + \frac{\sigma_1}{RD_2}\gamma_2\Big(\frac{31}{80}, \frac{13}{20}, \frac{4}{3}\Big) + \Omega_1\gamma_4\Big(-\frac{123}{80}, \frac{61}{20}, \frac{19}{30}, -\frac{11}{3}, -3\Big)\Big],$$

$$T_{17} = -\frac{19}{40} + \Omega_1\Big[\gamma_2\Big(-\frac{47}{80}, -\frac{11}{24}, -\frac{13}{12}\Big) + \frac{R_3}{RU}\gamma_2\Big(0, \frac{1}{16}, \frac{1}{3}\Big)$$
$$+ \frac{RD_1}{U}\gamma_2\Big(0, -\frac{15}{16}, \frac{13}{4}\Big) + \frac{\sigma_1}{RD_2}\gamma_2\Big(\frac{5}{8}, -\frac{7}{4}, -\frac{5}{3}\Big) + \Omega_1\gamma_4(\tfrac{3}{8}, -\tfrac{1}{2}, \tfrac{1}{3}, \tfrac{4}{3}, 2)\Big]$$

$$T_{18} = -\tfrac{9}{4} + \Omega_1\delta_2(0, -\tfrac{15}{8}, -\tfrac{1}{2}) \quad \text{and} \quad T_{19} = \tfrac{3}{2} + \Omega_1\gamma_2(0, \tfrac{5}{4}, 0).$$

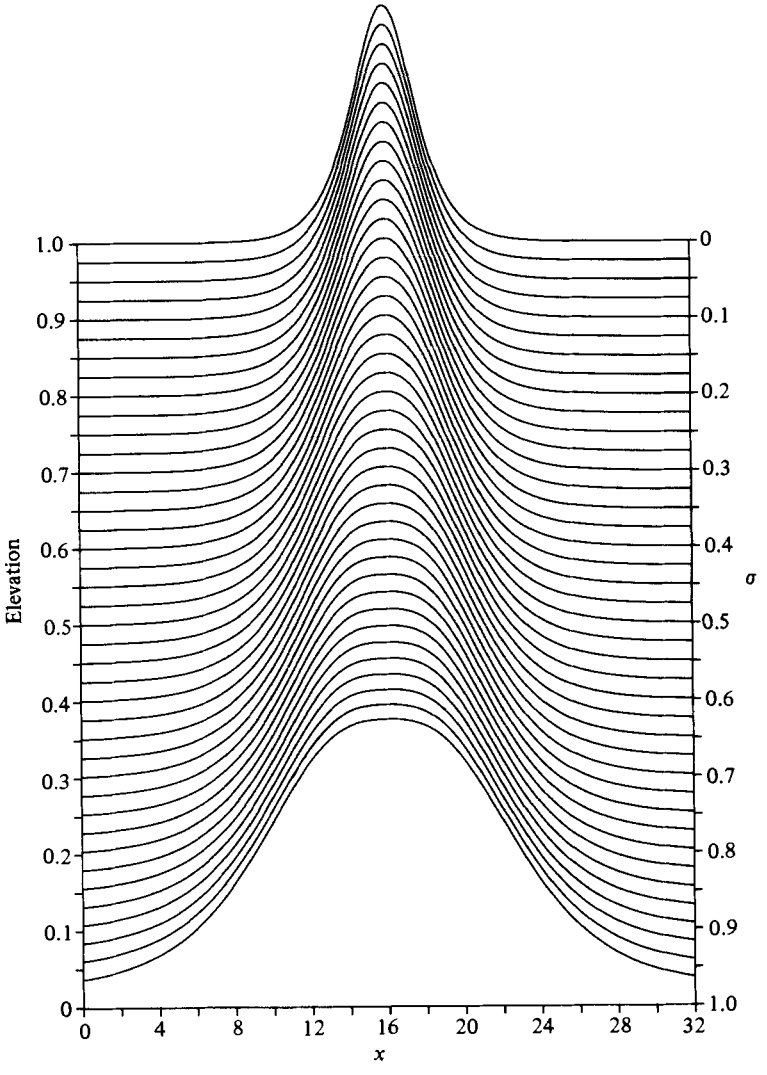

FIGURE 2. The elevation versus the space and σ of the amplitude 0.31 solitary wave. The third-order solution is used for $R = -1.8$. As σ increases, the wave becomes flatter.

2.3. *Run up*

The run up (maximum amplitude during the interaction) is given by

$$\text{run up} = \zeta(f = 1, g = 1)$$
$$= \epsilon_R + \epsilon_L + \lambda_1 \epsilon_R \epsilon_L + (2\lambda_1)^2 \epsilon_R \epsilon_L (\epsilon_R + \epsilon_L)\,[\tfrac{3}{8} + \Omega_1(\tfrac{1}{2}U + \tfrac{5}{8}R_2 D_2)]. \quad (20)$$

For two identical solitary waves (reflection) we have

$$\text{run up} = 2\epsilon_R + \lambda_1 \epsilon_R^2 + (2\lambda_1)^2 \epsilon_R^3 [\tfrac{3}{4} + \Omega_1(U + \tfrac{5}{4}R_2 D_2)]. \quad (21)$$

In figure 3 we plot the run up versus the amplitude for $R = -2.5$, and several values of σ. As σ increases, the run up diminishes.

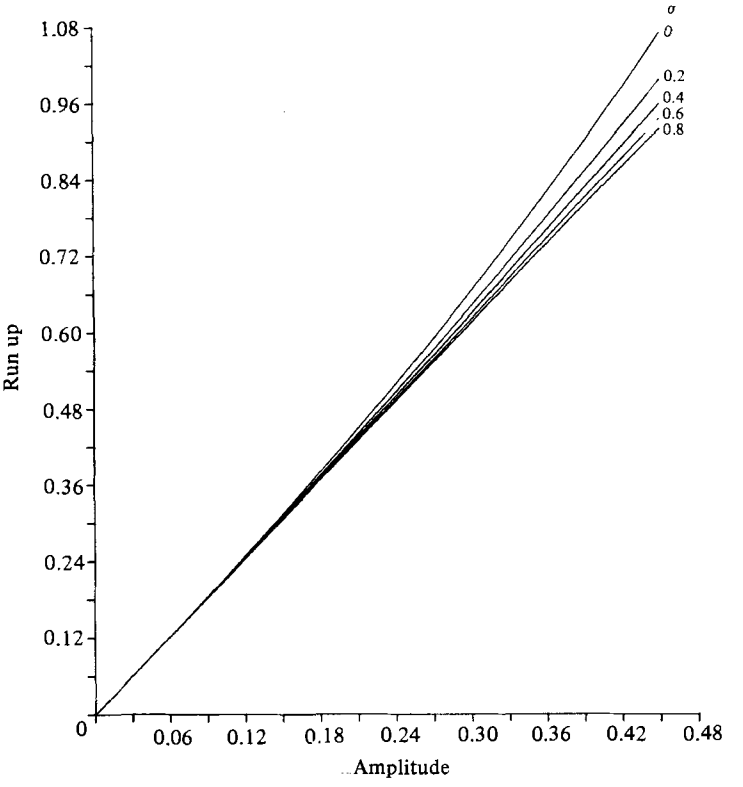

FIGURE 3. The third-order result for the run up of a head-on collision of two identical internal solitary waves versus the wave amplitude. $R = -2.5$; $\sigma = 0, 0.2, 0.4, 0.6, 0.8$.

2.4. *Phase shift and trailing wavetrain*

The phase shift is given by

$$\theta = \tfrac{1}{2}|\lambda_1|h_0\left(\frac{U\epsilon_L}{3D_2}\right)^{\frac{1}{2}}\left[\int_{-\infty}^{\eta}\left[1+2\lambda_1\epsilon_L(T_{20}g+T_{21})+\epsilon_R\left(2\lambda_1 T_{22}+9(1-\sigma)\frac{f}{U}\right)\right]g\,d\eta_1\right], \quad (22)$$

where $$T_{20} = \tfrac{3}{2}+\Omega_1\gamma_2(-\tfrac{3}{4}, 4, 3), \quad T_{21} = -\tfrac{7}{8}+\Omega_1\gamma_2(\tfrac{5}{8}, -3, -\tfrac{3}{2})$$

and $$T_{22} = -\tfrac{13}{4}+\Omega_1\gamma_2(0, -3, 0).$$

The term dependent on f in the θ-equation is classified as a non-uniform phase shift. It causes the emergent wave after a head-on collision to tilt backwards to its direction of motion. We study the slow time evolution of an asymmetric solitary wave by a similar procedure to that of paper 1. We use a reference frame centred in the solitary wave:

$$\xi = K\epsilon^{\frac{1}{2}}(x-C_R t), \quad \tau = K\epsilon^{\frac{3}{2}}C_R t, \quad 23$$

where $K^2 = 3aD_2/U$, and $a = \pm 1$ depending on $D_2 \gtrless 0$. Then C_R, ζ, W_1 and W_2 are expanded in power series in terms of ϵ and substituted in [eqn (3) $\pm$ (eqn (1) $-(\sigma/R)$ eqn (2))]. We find that the equation governing the difference between a symmetric and an asymmetric solitary wave is given by

$$2V_\tau+\frac{aD_2}{D_1}[(3S-1)V+V_{\xi\xi}]_\xi = 0. \quad (24)$$

This is identical with equation (67) of paper 1, if we let $\tau' = (aD_2/D_1)\tau$.

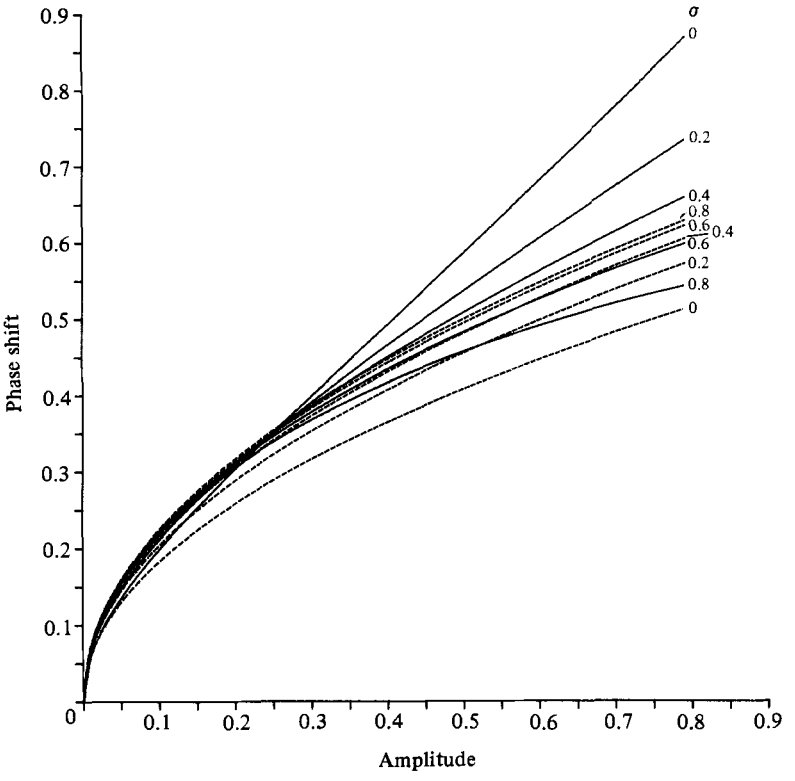

FIGURE 4. The phase shift after collision of two identical internal solitary waves versus the wave amplitude. $R = -2.5$; $\sigma = 0, 0.2, 0.4, 0.6, 0.8$. ----, first-order; ——, second-order.

The initial data $V(\xi, 0) = \gamma SS' = 9\epsilon^{\frac{3}{2}}(1-\sigma)(2\lambda_1)SS'/U$ allow us to determine $V(\xi, \tau')$. The solution is given by

$$V(\xi, \tau') = \tfrac{4}{9}\gamma S' + (\tfrac{1}{9}\gamma)\int_{-\infty}^{\infty} \mathrm{d}K\, \tilde{S}\, F(\xi, K)\, \mathrm{e}^{-\frac{1}{2}\mathrm{i}\tau'(K+K^3)+\mathrm{i}k\xi}, \tag{25}$$

where $\tilde{S} = 2K/\sinh \pi K$ and

$$F(\xi, K) = \mathrm{i}K(K^2-1) + 2\mathrm{i}S(\xi) + S'(\xi) + \frac{2K^2 S'(\xi)}{S(\xi)} \tag{26}$$

(see Jeffrey & Kakutani 1970; Berryman 1976, 1979). For large τ' and fixed ξ/τ', the above integral admits two stationary points given by

$$3K_0^2 = -\left[1 + \frac{2D_1\xi}{D_2 a\tau}\right]. \tag{27}$$

A bounded solution $V(\xi, \tau)$ exists for real K_0, i.e. for $2D_1\xi/D_2 a < -\tau$, and the asymptotic behaviour of the integral is given by

$$\left(\frac{8\pi}{3|K_0|\tau'}\right)^{\frac{1}{2}} \tilde{S}(K_0)\left[\left(1 + \frac{2K_0^2}{S(\xi_0)}\right)S'(\xi_0)\cos(\tau' K_0^3 - \tfrac{1}{4}\pi) + K_0(K_0^2 - 1 + 2S(\xi_0))\sin(\tau' K_0^3 - \tfrac{1}{4}\pi)\right]. \tag{28}$$

This represents a wavetrain (wavelet) that started with a profile $\gamma SS' - \frac{4}{9}\gamma S'$. In both

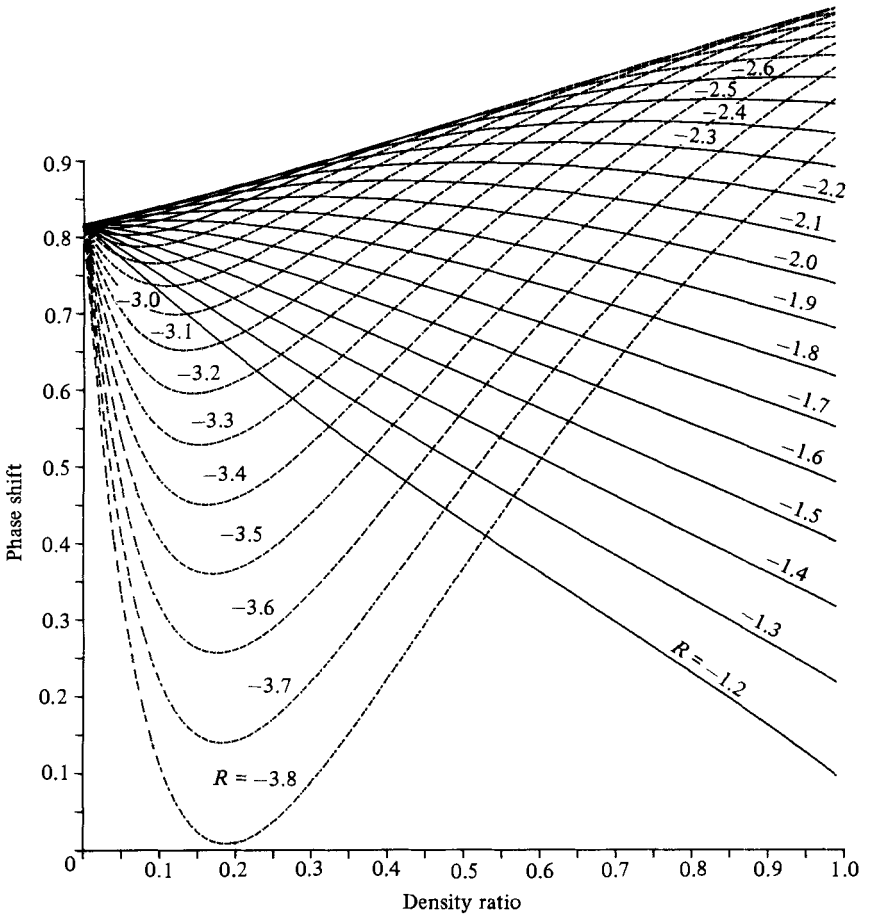

FIGURE 5. The second-order phase shift versus σ and R for the amplitude 0.31 solitary-wave reflection. R goes from -1.2 to -3.8. ——, $R = -1.2$–-2.6; – – – –, $R = -2.7$–-3.8.

cases $\sigma \gtrless R^2$ the wavetrain trails behind the symmetric solitary wave, and its amplitude diminishes in time as $t \to \infty$, owing to dispersion.

The term $\frac{4}{9}\gamma S'(\xi)$ in $V(\xi, \tau)$ adds to the uniform phase shift. Thus the total uniform phase shift of the right-going wave up to $O(\epsilon^{\frac{3}{2}})$ is

$$\Delta\theta = |2\lambda_1|\, h_0 \left(\frac{U\epsilon_{\mathrm{L}}}{3D_2}\right)^{\frac{1}{2}} [1 + (2\lambda_1)\,\epsilon_{\mathrm{L}}(\tfrac{1}{8} + \Omega_1\gamma_2(\tfrac{1}{8}, -\tfrac{1}{3}, \tfrac{1}{2})) + (2\lambda_1)\,\epsilon_{\mathrm{R}}(\tfrac{3}{4} + \Omega_1\gamma_2(0, 1, 0))]. \quad (29)$$

For two identical solitary waves (reflection) we have

$$\Delta\theta = |2\lambda_1|\, h_0 \left(\frac{U\epsilon_{\mathrm{R}}}{3D_2}\right)^{\frac{1}{2}} [1 + (2\lambda_1)\,\epsilon_{\mathrm{R}}(\tfrac{7}{8} + \Omega_1\gamma_2(\tfrac{1}{8}, \tfrac{2}{3}, \tfrac{1}{2}))]. \quad (30)$$

In figure 4 we plot the first- and second-order phase shift versus the wave amplitude. We notice that, as σ increases, the first-order contribution increases slowly, while the second-order part diminishes strongly. In figure 5 we plot the phase shift of an internal solitary wave of amplitude 0.31 versus R and σ.

2.5. *Energy consideration*

We now consider the time of change of the total energy in the wavetrain. This can be obtained by multiplying (24) by V and integrating from $-\infty$ to $+\infty$, i.e.

$$\left[\int_{-\infty}^{\infty} V^2 \,\mathrm{d}\xi\right]_\tau = -\frac{3D_2 a}{2D_1}\int_{-\infty}^{\infty} S' V^2 \,\mathrm{d}\xi. \tag{31}$$

Suppose that the wavetrain has not completely separated from the main wave and is riding on the tail of the latter, then for a right-going wave we are considering $S' > 0$. Since $D_2 a/D_1$ is positive, we see that

$$\left[\int_{-\infty}^{\infty} V^2 \,\mathrm{d}\xi\right]_\tau < 0. \tag{32}$$

This represents a decrease in energy of the wavetrain. Since the total energy in the fluid is conserved, we conclude that in the final phase of the evolution of the wavetrain (i.e. when it rides on the tail of the main wave) the main wave is gaining in energy at the expense of the wavetrain.

This energy transfer is manifested in recent numerical results on the head-on collision of two solitary waves at the surface of an infinite channel ($\sigma = 0$ case) (see Funakoshi & Oikawa 1982; Mirie 1980).

3. Head-on collision at the surface of an infinite channel

The solution obtained in §2 reduces (for $\sigma = 0$) to that of paper 1, and extends its solution in finding an energy transfer from the wavetrain to the main wave. Recently there have been several numerical calculations on the head-on collision between two solitary waves. We take this opportunity to review these results.

Because the head-on collision of two identical waves is equivalent to the reflection of one wave by a wall, we follow Maxworthy (1976) in referring to the head-on collision by wave–wall and wave–wave interactions.

Mirie & Su (1982) used a finite-difference method on the Su–Gardner (1969) set of equations. They studied both kinds of interactions. Funakoshi & Oikawa (1982) repeated Chan & Street's (1971) calculations by integrating the Euler equations by the same numerical method (MAC) developed by the latter authors to study the wave–wall interaction. However, Funakoshi & Oikawa used the ninth-order solution of Fenton (1972) with amplitudes ranging from 0.05 to 0.2 inclusive. Fenton & Rienecker (1982) integrated the general equations of motion using a Fourier method. They studied both kinds of interactions, and used the Fenton (1972) solution as initial data.

3.1. *The maximum run up during the interaction*

The second-order result of Byatt-Smith (1971) and Oikawa & Yajima (1973) agreed well with the numerical work only for small amplitudes. On the other hand, the third-order result of paper 1 showed excellent agreement for all the amplitudes considered (see figure 6).

3.2. *The dispersive wavetrain*

Maxworthy (1976) had reported a secondary wave trailing behind the solitary wave of amplitude 0.31, after reflection by a wall. The theory in paper 1 indicated the existence of this secondary wave as a dispersive wavetrain in both kinds of

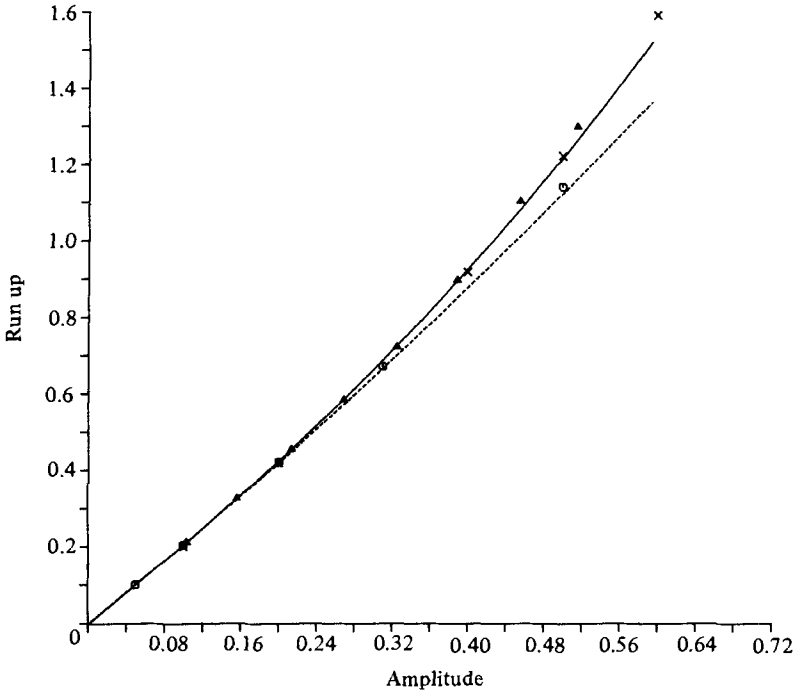

FIGURE 6. The run up of a head-on collision of two identical solitary waves at the free surface of an infinite channel versus the wave amplitude. – – – –, Byatt-Smith (1971) and Oikawa & Yajima (1973); ——, paper 1; ×, numerical results of Chan & Street (1971) and Funakoshi & Oikawa (1982); ○, Mirie & Su (1982); △, Fenton & Rienecker (1982).

interactions. Mirie & Su (1982) confirmed the existence of the wavetrain for the Su–Gardner equations and compared their results with the solution of paper 1. They have reported a wavetrain in both kinds of interactions, even for small-amplitude waves. Funakoshi & Oikawa (1982) confirmed the existence of the wavetrain in the Euler equations for the five amplitude cases they have integrated. They reported qualitative agreement with the theory. Fenton & Rienecker (1982) reported the existence, for amplitudes greater than 0.3, of a secondary wave in the general equations in the wave–wall interaction.

The third-order theory suggests that the wavetrain amplitude decays as the reflected wave propagates away from the centre of interaction. This was confirmed by Mirie & Su, where they have extended their range of integration twice and compared their numerical results with paper 1. Funakoshi & Oikawa have plotted in their figure 3 the dispersion of the wavetrain at different times up to 35.5 (non-dimensional time). Their results are similar to those of Mirie & Su. Unfortunately, Fenton & Rienecker were unable to study the slow time evolution of the wavetrain for larger times, owing to their numerical method.

3.3. *Increase in wave speed of the main reflected wave*

Maxworthy reported that the wave travels faster after reflection. However, he gave no further details. Funakoshi & Oikawa reported that there is a slight increase in the wave speed, and they noted that the speed is measured from the position of the slowly varying crest. In a private communication, Funakoshi & Oikawa showed that the speed of the crest is higher than the incoming wave just after collision, but decreases

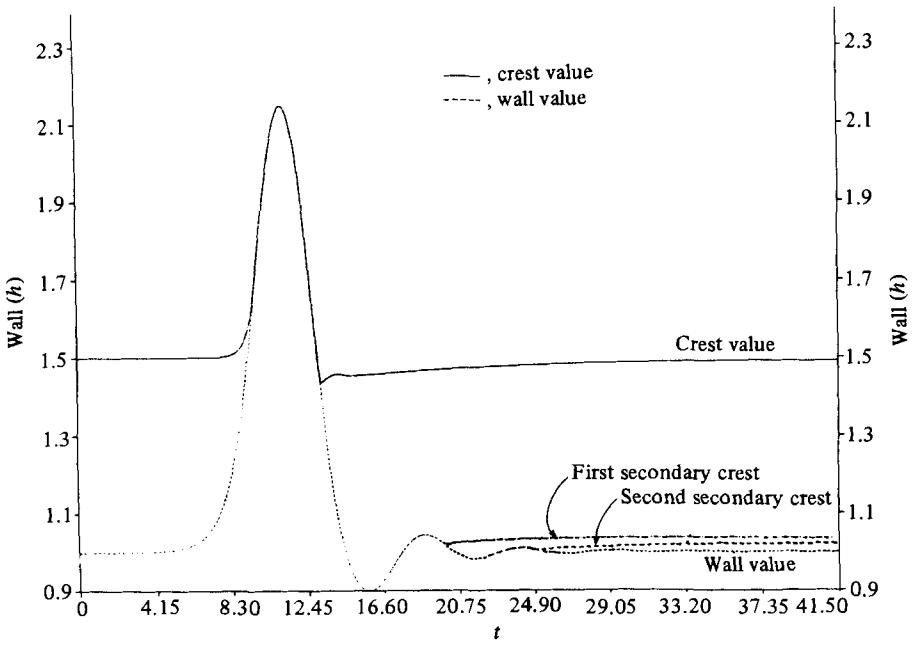

FIGURE 7. The crest value versus time for the amplitude 0.3 case of a solitary wave at the surface being reflected by a vertical wall (Mirie 1980; Mirie & Su 1982). ----, water level at the wall.

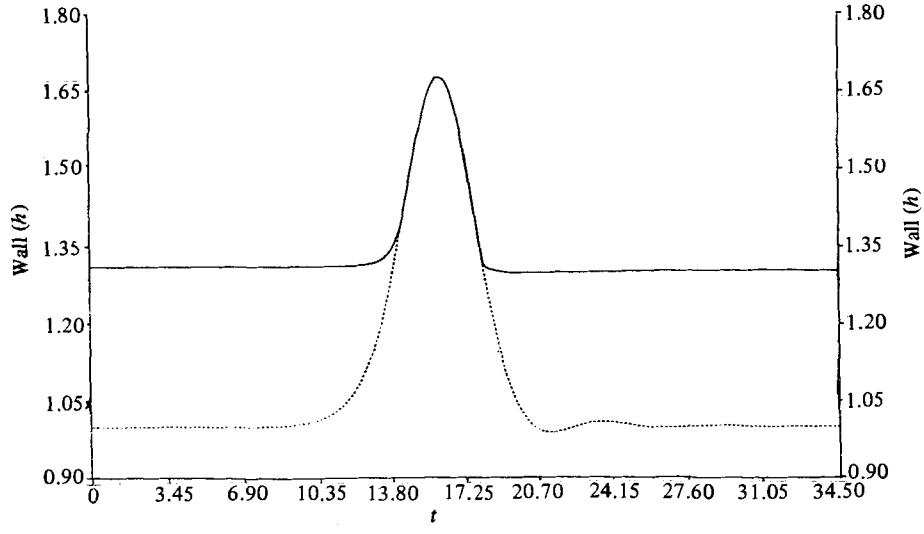

FIGURE 8. Same as figure 7 for the amplitude 0.31 case.

gradually as time elapses, and finally oscillates around the latter. Fenton & Rienecker suggested an empirical third-order relation in amplitude. Based on the numerical results of Funakoshi & Oikawa and our own, we believe that the integration time of Fenton & Rienecker is too short to give any useful information concerning the state of solitary waves long after collision.

The time of integration as well as the waves considered varied in the three numerical studies. Fenton & Rienecker's time of integration extends till the reflected wave returned to its initial position in all the cases they considered except the

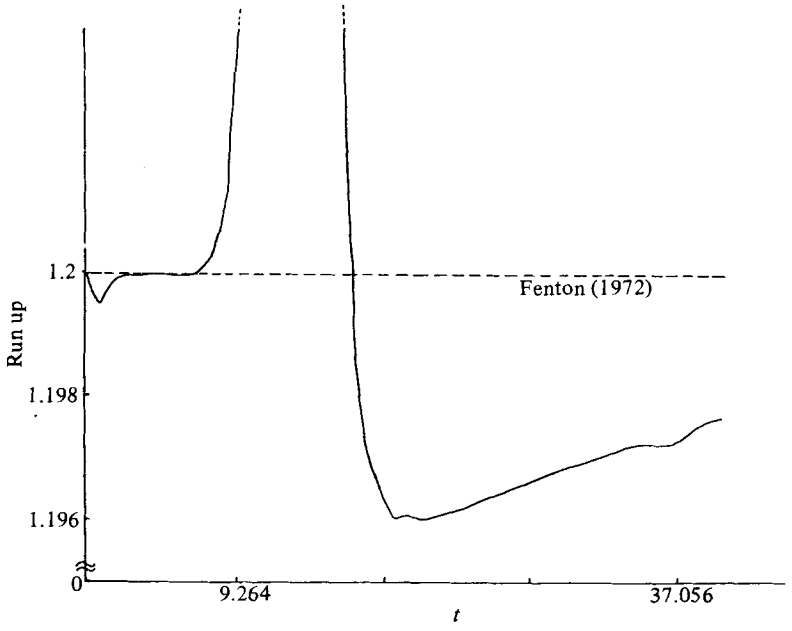

FIGURE 9. The crest value versus time for the amplitude 0.2 case of a solitary wave at the surface being reflected by a vertical wall (Funakoshi & Oikawa 1982). This figure comes from a private communication from the above authors.

multiple-reflection case. Funakoshi & Oikawa have a detailed study of the case of amplitude 0.2, and their time of integration is about three times that of Fenton & Rienecker. The integration time of Mirie & Su is comparable to that of Fenton & Rienecker for the wave–wave interaction, but is more than six times longer in the amplitude 0.5 case considered.

3.4. *Decrease in the amplitude of the main reflected wave*

Mirie (1980) depicted the amplitude versus time for five amplitude cases ranging from 0.05 to 0.5 (see figures 9(*a*, *b*) there or figures 7 and 8 in this paper). In the 0.5 amplitude case Mirie & Su considered, they extended their range of integration so as to allow the wavetrain to detach from the main reflected wave. They have found that the decrease in amplitude slowly diminished; however, the amplitude of the main wave did not regain its initial value. They have concluded that the wave did not recover 100 % of its initial profile and had lost about 2 % of its amplitude and energy. They also noted that at the end of integration this (real) loss lies beyond the accuracy of the third-order calculations. We shall return to this at the end of this section. Funakoshi & Oikawa considered the amplitude 0.2 case in greater detail where they presented the deviation of the reflected wave from the initial wave at any point and at several times. In their figure 3 the decrease in crest amplitude is 0.0036, at time 23.9. While this decrease is 0.0032 at time 29.6 and 0.0023 at time 35.5, and it is still evolving at the end of this plot. The difference gets smaller as the wave evolves away from the wall. Fenton & Rienecker considered in great detail the two kinds of interactions. They have investigated the decrease in wave amplitude, proposed an empirical formula ($0.4\epsilon^3$), and interpreted their results on the decrease in amplitude as a third-order effect not accounted for by paper 1. Figure 9 of this paper, kindly supplied by Funakoshi & Oikawa for the amplitude 0.2 case, describes the variation

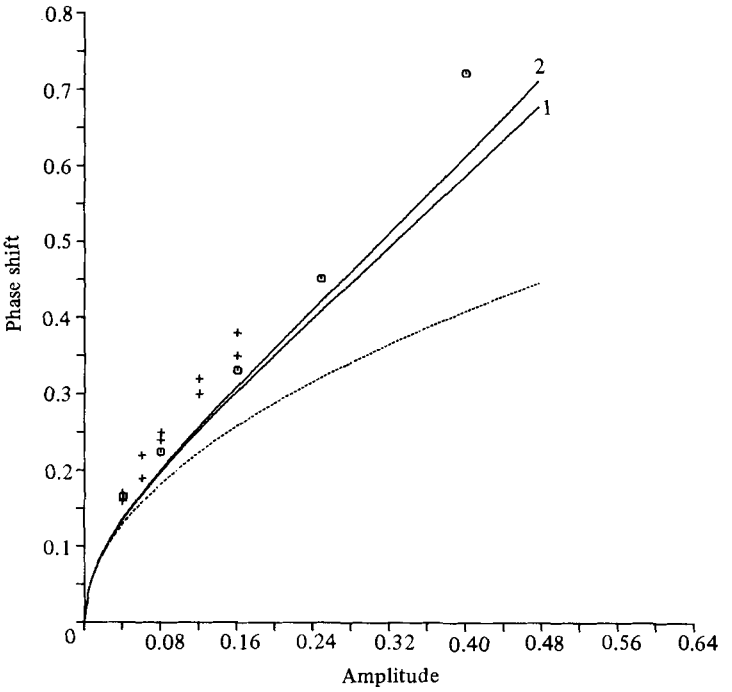

FIGURE 10. The phase shift after reflection at the free surface of an infinite channel versus the wave amplitude. – – – –, Oikawa & Yajima (1973) and implicit results from Byatt-Smith (1971); ——1, paper 1; ——2, △, from Mirie & Su (1982); +, numerical results of Funakoshi & Oikawa (1982).

of the amplitude of the main wave throughout their time of integration. Figures 7–9 agree with Fenton & Rienecker, when the wave is close to the wall, that the decrease is a third-order effect. But as the wave proceeds away from the wall this dip in amplitude diminishes, and the wave starts slowly to recover its initial profile. These figures demonstrate also that there is an energy transfer from the wavetrain to the main wave. It seems that the integration time used by Fenton & Rienecker is not long enough to catch the slow recovery of the main waves after their collision. This lack of sufficient time in integration may also account for erroneously large phase-shift data as will be discussed in §3.5.

Our calculation shows that the main wave will regain its original form up to third-order accuracy. However, this will be so only if we wait long enough for the wavetrain to be completely separated from the main wave. Throughout the separation process the apparent energy loss will be slowly transferred back to the main wave as shown in (32) and figures 7–9. For relatively large-amplitude waves we expect a real energy loss to persist even after a complete separation has occurred. (See figure 3 of Mirie & Su 1982). This real energy loss, however, will be higher than third order in amplitude.

3.5. *The phase shift*

The numerical results of Mirie & Su and Funakoshi & Oikawa, which are based on a sufficiently long time after reflection, indicate that the phase shift is amplitude dependent and does not depend on any location in this interval (see figure 10). The numerical results also agree with the theoretical prediction. However, before the time when the wavetrain is completely separated from the main wave, the phase shift will

depend on the position where it is measured, simply because the amplitude and thus the wave speed of the main wave have not settled down to the fixed values yet. The discrepancies in phase shifts between experiment (both laboratory and computer) and theory is mainly due to the fact that the values obtained in experiments are taken at times when the solitary wave is still interacting with the wavetrain riding on its tail. This evolution process can escape one's attention easily in comparison with the relatively dramatical collision process of two main waves. Furthermore, the former process carries on long after the two main waves are well separated in space.

This research has been supported by the Department of Mathematical Sciences at UPM, the National Science Foundation, Fluid Mechanics Program, and by the Office of Naval Research, U.S. Navy. We acknowledge the use of Reduce 2 language. We are grateful for the kindness of Professors Mitsuaki Funakoshi and Masayuki Oikawa for supplying figure 9. Mirie wishes to express his appreciation for all the help and support of H.R.H. Prince Salman Bin Abdul-Aziz Al-Saud.

Appendix A

Substituting the perturbation expansion (6) in [eqn (3)+eqn (1)$-(\sigma/R)$ eqn (2)] we obtain a power series in ϵ, which we denote by the α-equation. We use the notation given in (7) and recast each order of ϵ alone.

$O[\epsilon] = 0$:

$$\alpha_{0\eta} = 0, \quad \beta_{0\xi} = 0. \tag{A 1}$$

$O[\epsilon^2] = 0$:

$$4LD_1\alpha_{1\eta} + K\alpha_{0\xi}[D_1(4L\theta_{0\eta} - 2a\lambda_1) + D_2(3\alpha_0 - \beta_0)] - LD_2\beta_{0\eta}(\alpha_0+\beta_0) + \tfrac{1}{3}U(K^3\partial_\xi^3 - 2L^3\partial_\eta^3)(\alpha_0+\beta_0) = 0. \tag{A 2}$$

$O[\epsilon^3] = 0$:

$$\begin{aligned}
&4LD_1\alpha_{2\eta} + K\alpha_{1\xi}[D_1(4L\theta_{0\eta} - 2a\lambda_1) + D_2(3\alpha_0 - \beta_0)] \\
&\quad + L\alpha_{1\eta}[2D_1 b\lambda_1 + D_2(3\alpha_0 - \beta_0)] - D_2(\alpha_0+\beta_0)(K\partial_\xi + L\partial_\eta)\beta_1 \\
&\quad - L\beta_{0\eta}[2L^2\sigma_1\beta_{0\eta\eta} + \tfrac{1}{3}UK^3\psi_{0\xi\xi\xi} + D_2(K\psi_{0\xi}(\alpha_0+\beta_0) + \alpha_1 + \beta_1)] \\
&\quad + K\alpha_{0\xi}[-\sigma_1(K^2\alpha_{0\xi\xi} + L^2\beta_{0\eta\eta}) - \tfrac{2}{3}UL^3\theta_{0\eta\eta\eta} \\
&\quad + D_1(4L\theta_{1\eta} + 2bL\lambda_1\theta_{0\eta} - 2a^2\lambda_2) + D_2(L\theta_{0\eta}(3\alpha_0 - \beta_0) + 3\alpha_1 - \beta_1)] \\
&\quad + K^3\alpha_{0\xi\xi\xi}(\tfrac{1}{2}Ua\lambda_1 - \sigma_1\beta_0) - UK^2\alpha_{0\xi\xi}\theta_{0\eta\eta} \\
&\quad + L^3\beta_{0\eta\eta\eta}(\tfrac{1}{2}Ub\lambda_1 - \sigma_1(\beta_0 + 2\alpha_0) + UK\psi_{0\xi}) \\
&\quad + \tfrac{1}{3}U(K^3\partial_\xi^3 - 2L^3\partial_\eta^3)(\alpha_1 - \beta_1) + \tfrac{1}{30}U_3(-K^5\partial_\xi^5 + \tfrac{3}{2}L^5\partial_\eta^5)(\alpha_0 - \beta_0) \\
&\quad + 2R_1\sigma_1(K\partial_\xi + L\partial_\eta)(\alpha_0 p_0) + \tfrac{1}{6}R_1R_2(-K^3\partial_\xi^3 + 2L^3\partial_\eta^3)(\alpha_0 p_0) = 0.
\end{aligned} \tag{A 3}$$

$O[\epsilon^4]$: secular terms only

These terms determine the arbitrary function $F_2(\xi)$ resulting from integrating the local terms in α_2. They were assembled with the aid of Reduce 2 (an algebraic-manipulation computer language developed by Hearn 1973). We have

$$F_2'' + (3f-1)F_2 = F_2'' - \frac{f'''F_2}{f'} = [2\lambda_3(2\lambda_1)^{-3} - [1]]f + [2]f^2 + [3]f^3 + [4]f^4, \tag{A 4}$$

where

$$[1] \equiv \tfrac{55}{56} - \frac{\sigma R_1^2 R_2^2}{70 R U^3}(4R_3 + 29RU),$$

$$[2] \equiv -\tfrac{393}{160} + \Omega_1\Big[\gamma_2\Big(-\frac{63}{16}, \frac{21}{10}, \frac{3}{2}\Big) + \frac{R_3}{RU}\gamma_2\Big(-\frac{9}{5}, \frac{57}{20}, 0\Big) + \frac{RD_1}{U}\gamma_2\Big(0, \frac{33}{8}, 0\Big) + \frac{\sigma_1}{RD_2}\gamma_2\Big(\frac{15}{8}, 0, 0\Big) + \Omega_1\gamma_4\Big(-\frac{27}{8}, +\frac{15}{2}, \frac{9}{2}, -12, -6\Big)\Big],$$

$$[3] \equiv \tfrac{201}{16} + \Omega_1\Big[\gamma_2\Big(\frac{141}{16}, \frac{19}{8}, -\frac{7}{2}\Big) + \frac{R_3}{RU}\gamma_2\Big(6, -\frac{83}{8}, -4\Big) + \frac{RD_1}{U}\gamma_2\Big(0, -12, -\frac{21}{2}\Big) + \frac{\sigma_1}{RD_2}\gamma_2\Big(-\frac{71}{8}, \frac{15}{2}, 0\Big) + \Omega_1\gamma_4\Big(\frac{93}{32}, -\frac{51}{2}, -11, 30, 18\Big)\Big]$$

and

$$[4] \equiv -\tfrac{591}{64} + \Omega_1\Big[\gamma_2\Big(-\frac{339}{64}, -\frac{169}{32}, -\frac{19}{8}\Big) + \frac{R_3}{RU}\gamma_2\Big(-\frac{9}{2}, \frac{63}{8}, \frac{7}{2}\Big) + \frac{RD_1}{U}\gamma_2\Big(0, \frac{243}{32}, \frac{51}{4}\Big) + \frac{\sigma_1}{RD_2}\gamma_2\Big(\frac{243}{32}, -\frac{33}{4}, -\frac{5}{2}\Big) + \Omega_1\gamma_4\Big(-\frac{279}{32}, \frac{153}{8}, \frac{29}{4}, -\frac{35}{2}, -\frac{15}{2}\Big)\Big],$$

where Ω_1, σ_1, γ_2, γ_4, R_1, R_2, R_3, U and D_2 are given in (7). Setting $2\lambda_3 = (2\lambda_1)^3[1]$, then $F_2 = m_1 f + m_2 f^2 + m_3 f^3$, where

$$m_3 = -\tfrac{2}{15}[4], \quad m_2 = -\tfrac{1}{30}(16[4] + 15[3]) \quad \text{and} \quad m_1 = \tfrac{2}{3}[2] + [3] + \tfrac{16}{15}[4].$$

Appendix B

The third-order solitary-wave solution can be obtained from (18) by setting $g = 0$. This solution extends by one order that of Koop & Butler (1981), which was verified by Gear & Grimshaw (1983). Koop & Butler proposed a second-order extended KdV equation given by

$$\zeta_t + C_0[\zeta + \tfrac{1}{2}C_1\zeta^2 + C_2\zeta_{xx} + C_3\zeta_{xxxx} + C_4\zeta\zeta_{xx} + C_5\zeta^3 + C_6\zeta_x^3]_x = 0.$$

Their solution was put in terms of the C_i coefficients. Here we list the relationships between the C_i and the notation we used in (7):

$$\frac{C_0^2}{gh_0} = C^2 = \frac{1-\sigma}{D_1}, \qquad C_1 = \frac{3D_2}{2D_1}, \quad C_2 = \frac{U}{6D_1},$$

$$C_3 = \frac{U_3}{90D_1} + \frac{U^2}{24D_1^2}, \qquad C_4 = \frac{\sigma-1}{6D_1} + \frac{7UD_2}{12D_1^2},$$

$$C_5 = \frac{1-\sigma R^{-3}}{D_1} + \frac{7D_2^2}{8D_1^2}, \qquad C_6 = \frac{\sigma-1}{12D_1} + \frac{17UD_2}{48D_1^2}.$$

The wavenumber is related to the C_i by

$$h_0 K = \Big(\frac{3\epsilon_R D_2}{U}\Big)^{\frac{1}{2}}[1 + 2\lambda_1\epsilon_R T_5] = \Big(\frac{\epsilon_R C_1}{3C_2}\Big)^{\frac{1}{2}}\Big[1 + \epsilon_R\Big(\frac{C_6}{12C_2} + \frac{3C_5}{4C_1} - \frac{C_4}{24C_2} - \frac{5C_3C_1}{24C_2^2}\Big)\Big].$$

And T_7 in (18) is related to the C_i by

$$2\lambda_1 T_7 = -\frac{C_6}{2C_2} + \frac{3C_5}{2C_1} - \frac{3C_4}{4C_1} + \frac{5C_3C_1}{4C_2^2}.$$

REFERENCES

BERRYMAN, J. G. 1976 Stability of solitary waves in shallow water. *Phys. Fluids* **19**, 771–777.

BERRYMAN, J. G. 1979 A reply to a comment by R. Van Dooren. *Phys. Fluids* **22**, 1588–1589.

BYATT-SMITH, J. G. B. 1971 An integral equation for unsteady surface waves and a comment on the Boussinesq equations. *J. Fluid Mech.* **49**, 625–633.

CHAN, R. K. C. & STREET, R. L. 1971 A computer study of finite amplitude water waves. *J. Comp. Phys.* **6**, 68–94.

FENTON, J. D. 1972 A ninth-order solution for the solitary wave. *J. Fluid Mech.* **53**, 257–271.

FENTON, J. D. & REINECKER, M. M. 1982 A Fourier method for solving nonlinear water-wave problems: application to solitary-wave interactions. *J. Fluid Mech.* **118**, 411–443.

FUNAKOSHI, M. & OIKAWA, M. 1982 A numerical study on the reflection of a solitary wave in shallow water. *J. Phys. Soc. Japan* **51**, 1018–1026.

GEAR, J. A. & GRIMSHAW, R. 1983 A second-order theory for solitary waves in shallow fluids. *Phys. Fluids* **26**, 14–29.

HEARN, A. C. 1973 *Reduce 2 User's Manual.* University of Utah.

KAKUTANI, T. & YAMASAKI, N. 1978 Solitary waves in a two-layer fluid. *J. Phys. Soc. Japan* **45**, 674–679.

KOOP, C. G. & BUTLER, G. 1981 An investigation of internal solitary waves in a two-fluid system. *J. Fluid Mech.* **112**, 225–251.

JEFFREY, A. & KAKUTANI, T. 1970 Stability of the Burgers shock wave and the Korteweg de Vries soliton. *Indiana Univ. Math. J.* **20**, 463–468.

LONG, R. R. 1956 Solitary waves in the one- and two-fluid systems. *Tellus* **8**, 460–471.

MAXWORTHY, T. 1976 Experiments on collisions between solitary waves. *J. Fluid Mech.* **76**, 467–490.

MILES, J. W. 1979 Internal solitary waves I. *Tellus* **31**, 456–462.

MILES, J. W. 1980 Solitary waves. *Ann. Rev. Fluid Mech.* **12**, 11–43.

MILES, J. W. 1981 Internal solitary waves II. *Tellus* **33**, 397–401.

MIRIE, R. M. 1980 Collisions of solitary waves. Ph.D. thesis, Brown University.

MIRIE, R. M. & SU, C. H. 1982 Collisions between two solitary waves. Part 2. A numerical study. *J. Fluid Mech.* **115**, 475–492.

OIKAWA, M. & YAJIMA, N. 1973 Interactions of solitary waves. A perturbation to nonlinear systems. *J. Phys. Soc. Japan* **34**, 1093–1099.

SEGUR, H. & HAMMACK, J. L. 1982 Soliton models for long internal waves. *J. Fluid Mech.* **118**, 285–304.

SU, C. H. & GARDNER, C. S. 1969 Korteweg de Vries equation and generalization. III. Derivation of the Korteweg de Vries equation and Burgers equation. *J. Math. Phys.* **10**, 536–539.

SU, C. H. & MIRIE, R. M. 1980 On head-on collision between two solitary waves. *J. Fluid Mech.* **98**, 509–525.